Astrocytic control in *in vitro* and simulated neuron-astrocyte networks

Barbara Genocchi
barbara.genocchi@tuni.fi
Faculty of Medicine and Health Technology, Tampere University
Tampere, Finland

Annika Ahtiainen
annika.ahtiainen@tuni.fi
Faculty of Medicine and Health Technology, Tampere University
Tampere, Finland

Michael T. Barros
michael.barros@tuni.fi
School of Computer Science and Electronic Engineering, University of Essex
Colchester, Essex, UK

Jarno M.A. Tanskanen
jarno.tanskanen@tuni.fi
Faculty of Medicine and Health Technology, Tampere University
Tampere, Finland

Jari Hyttinen
jari.hyttinen@tuni.fi
Faculty of Medicine and Health Technology, Tampere University
Tampere, Finland

Kerstin Lenk
kerstin.lenk@tugraz.at
Institute of Neural Engineering, Graz University of Technology
Graz, Austria

ABSTRACT

Astrocytes are involved in the information propagation in the brain by interacting with neurons. Computational modeling helps to study the underlying mechanisms for this communication deeply. In this work, we aimed to analyze how the number of astrocytes and the resulting astrocytic network structure affects neuronal activity. Therefore, we conducted *in vitro* experiments with microelectrode arrays and simulations with our previously published computational neuron-astrocyte network model side-by-side. In those, we included neuronal cultures without supplemented astrocytes and three conditions with co-cultures where different amounts of astrocytes were added. We then conducted a cross-correlation analysis between the single-channel spike trains and a graph analysis, which included the mean degree, mean shortest path, and the number of nodes, based on the highly correlated channels. Furthermore, we combined the cross-correlation network analysis of the simulated data and the structure of the astrocyte topology. Our experimental results showed that the spike rate was very variable and higher in cultures without added astrocytes than overall in co-cultures. In the co-cultures, the activity was elevated with an increasing number of astrocytes. Additionally, the spike rate was correlated with the mean degree of the neuronal network. This correlation was smaller with larger numbers of astrocytes in the culture. The simulations showed that the most active neurons were localized in the center of the network, which were, however, not always the most connected ones. The astrocytic activation was mainly driven by the vicinity to highly active neurons rather than from the activation through gap junctions. To conclude, the co-cultures with added astrocytes showed stabilization of neuronal activity. Furthermore, increasing the number of astrocytes led to a higher neuronal activity, indicating a feedback excitation loop between astrocytes and neurons.

KEYWORDS

neurons, astrocytes, simulations, *in vitro* microelectrode arrays, graph analysis

ACM Reference Format:
Barbara Genocchi, Annika Ahtiainen, Michael T. Barros, Jarno M.A. Tanskanen, Jari Hyttinen, and Kerstin Lenk. 2021. Astrocytic control in *in vitro* and simulated neuron-astrocyte networks. In *The Eight Annual ACM International Conference on Nanoscale Computing and Communication (NANOCOM '21), September 7–9, 2021, Virtual Event, Italy.* ACM, New York, NY, USA, 7 pages. https://doi.org/10.1145/3477206.3477458

1 INTRODUCTION

In the field of *Molecular Communications*, biophysical interactions between cells are modelled as a communication system [10, 17, 18]. In the brain, astrocytes and neurons form tight networks and exchange information. Neurons and astrocytes communicate in a close feedback loop, which serves as a mechanism for synaptic activity regulation. Astrocytes play an essential role in controlling neuronal activity, and their impairment can lead to neurological diseases. For example, astrocyte dysfunctions have been found in epilepsy, Alzheimer's disease, brain tumors, major depressive disorder, and Down syndrome [5].

Computational models are used to understand biophysical pathways and to support experiments. Various types of astrocyte models with different levels of details – from subcellular to network level – have been developed to study intra- and intercellular mechanisms of astrocytes and their communication to neurons [reviewed in 12]. For example, Amiri et al. [1] introduced a model including 50 pyramidal neurons, 50 interneurons and 50 astrocytes. Inhibitory and excitatory neurons were linked in pairs to their neighbors and one astrocyte. The latter also was connected with one neighboring astrocyte via gap junctions (GJs). With the model, the authors demonstrated that increasing the astrocytic coupling strength to the excitatory and inhibitory neurons resulted in decreased synchronized neuronal oscillations.

In this work, we explored how astrocytes affect neuronal network activity using a multi-modal analysis comprised of both *in vitro* and computational modeling. For that, we recorded neuronal activity from neuronal cultures without added astrocytes as well as neuron-astrocytes co-cultures plated on microelectrode arrays (MEAs). The co-cultures were composed of different neuron-astrocyte ratios to study how the amount of astrocytes affects neuronal activity. Moreover, we aimed to study how the astrocytic network topology influences the activity. For this, we used a mathematical neuron-astrocyte network model developed by Lenk et al. [10, 11] and Genocchi et al. [7]. To understand the role of neuron-astrocyte connection in both experimental and simulation data, we performed a graph analysis based on the correlations between the spike trains from selected neurons as well as on the simulated astrocytic topology. *Molecular Communications* seek efforts that unite the analysis of intercellular communication mechanisms. Our model that analyzes different brain cell types within the same graph analysis on network structure and activity contributes to that work.

2 BACKGROUND AND RELATED WORK

Biological relevance. The intercommunication between neuronal networks and astrocytes regulates cognitive functions [14]. A pre- and a postsynaptic neuron can be enwrapped by an astrocyte and build together the so-called tripartite synapse (Fig. 1) [2]. Triggered by incoming action potentials, the presynaptic neuron releases neurotransmitters like glutamate to the synaptic cleft. Glutamate binds to the metabotropic glutamate receptors (mGluR) at the astrocyte's cell membrane. Consequently, inositol 1,4,5-trisphosphate (IP_3) is released from the endoplasmic reticulum followed by calcium (Ca^{2+}) elevations in the cytosol. The increasing Ca^{2+} levels trigger the opening of further IP_3 channels leading to a Ca^{2+}-induced Ca^{2+} release (CICR). Linked with the Ca^{2+} elevations is a release of gliotransmitters like glutamate, D-serine, or adenosine triphosphate (ATP) [3, 13]. Astrocytes diffuse gliotransmitters and IP_3 with a short-distance communication through GJs [14]. Thus, astrocytic network connectivity is crucial for activity control and network synchronization.

Computational network model. Recently, we have published a neuron-astrocyte network model called INEXA [7, 10, 11], which represents a computational equivalent of *in vitro* neuron-astrocyte co-cultures on MEAs. The neurons can be either excitatory or inhibitory. The astrocytes are connected to the excitatory synapses and to neighboring astrocytes by GJs. In this framework, astrocytes control the neuronal activity of the connected synapse through local calcium dynamics and the uptake and release of excitatory and inhibitory gliotransmitters. Local astrocytic calcium dynamics are summed into global calcium dynamics, simulating the calcium wave propagation through GJs. The novelty of the INEXA model was the simulation of the communication between astrocytes and neurons in a biophysically plausible network topology. In Lenk et al. [11], we investigated the influence of different ratios of astrocytes on neuronal network activity. The results showed that astrocytes stabilize neuronal activity with a delicate balance between excitation and inhibition. In Genocchi et al. [7], we further explored the role of GJ coupling on this balancing effect. Our simulation results indicated that a highly coupled astrocytic network was more

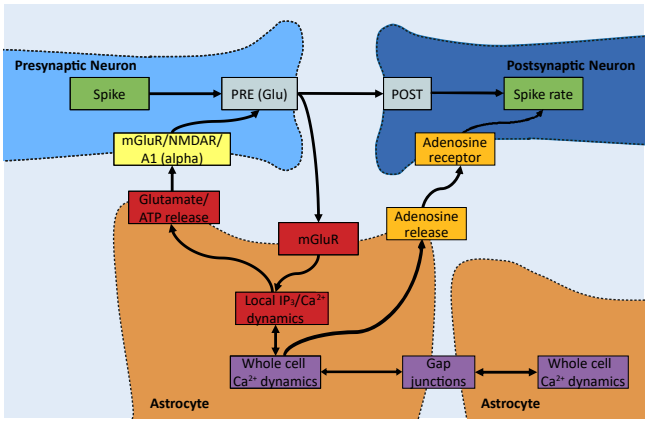

Figure 1: Schematic of a pre- and a postsynaptic neuron and an adjacent astrocyte. Figure adapted from Lenk et al. [11].

effective in decreasing the spike rate of the neurons compared to the networks with fewer GJs on average. In Lenk et al. [10], we extended the network from a planar topology to a 3D network model and simulated different astrocytic network topologies modifying the maximum distance between astrocytes. The results from the analysis of the 3D network revealed that larger connection distances between astrocytes centralized the information flow in the astrocytic network.

Molecular communications in neuron-astrocyte networks. An effort to describe the communication pathways between neurons and astrocytes from the viewpoint of *Molecular Communications* has also been made. In Valenza et al. [18], the authors implemented a network communication model between artificial spiking neurons and astrocytes. The tripartite synapse was described as a nonlinear transistor-like model. Their model showed that the presence of astrocytes in the network created subgroups of neurons with polychronic activity. This particular pattern of activity is considered to be the basis of the network memory. In Taynnan Barros et al. [17], communication in different types of cells has been studied. The authors considered excitable cells (smooth muscle cells), non-excitable cells (epithelial cells), and hybrid cells (astrocytes). The communication in this model happens through Ca^{2+} signaling through GJs. Their results highlight that the complex intracellular behavior as well as the size and structure of connections between the cells (i.e., GJ coupling) can impact the communication performance in the different models.

3 METHODS

Cell culturing. Co-cultures were established by combining rat primary cortical astrocytes (N7745100; Thermo Fisher Scientific) and primary rat cortex neurons (A1084001; Thermo Fisher Scientific) at specified ratios. Astrocytes, before MEA plating, were cultured until confluency and subsequently treated with Cytosine b-D-arabinofuranoside (ara-c; C1768; 2.5 μM; Sigma-Aldrich) for five days to terminate further astrocyte proliferation. On the day of MEA plating, neurons and astrocytes were centrifuged and counted as stated in the Thermo Fisher Scientific protocols. The number of neurons was always kept constant (80,000 neurons per MEA). The

number of astrocytes per MEA was adjusted to achieve different neuron-astrocyte co-culture ratios. The co-culture ratios used were 90:10, 80:20, and 70:30 percent, where the first number represents the percentage of plated neurons and the second number percentage of plated astrocytes. In addition to co-cultures, cultures with only neurons (NS) were prepared without any separately added astrocytes. Half the volume of the medium was refreshed every 2-3 days and always completely refreshed after MEA recordings (see next paragraph). Neuron-astrocyte co-cultures were cultured in neurobasal plus medium supplemented with 2% B-12 Plus supplement, 1% P/S, 1% GlutaMAX, and 1% sodium pyruvate. NS cultures were cultured in the cell culture media as suggested in the Thermo Fisher Scientific protocols.

MEA preparation and recording. The day before cell plating, all sterilized MEAs (n=28) were coated with Poly-D-Lysine (0.1 mg/ml; Thermo Fisher Scientific) for 1 hour. The MEAs were washed three times with ultrapure water, dried, and incubated with laminin (L2020; 20 μg/ml; Sigma-Aldrich) overnight at +4 °C. The following day, laminin was aspirated just before the plating. MEAs used in this study were either standard or thin 60-electrode MEAs (60MEA200/30iR; Multi Channel Systems MCS GmbH, Reutlingen, Germany). Raw signals were recorded at 28 days *in vitro* (DIV) at a sampling rate of 25 kHz for 5 minutes using a MEA2100-System and the Multi Channel Experimenter software. The raw signals were filtered and sorted with a tool called Wave Clus for MATLAB (R2009b or higher) [4]. We used a second-order bandpass elliptic filter in the range of 300 - 3000 Hz. Positive and negative spikes were detected when they exceeded the threshold of $\pm 5\sigma$, where σ is the standard deviation of the filtered signal.

Neuronal and neuron-astrocyte network simulations. Planar neuronal and neuron-astrocyte networks were simulated using the INEXA model [11]. The use of a planar network topology better resembles the *in vitro* cell distribution on a MEA. To reproduce the experimental setup, we simulated topologies with 250 neurons (200 excitatory and 50 inhibitory) without any astrocytes and with different numbers of astrocytes to reflect the plated ratios (i.e., ratio 90:10, 28 astrocytes; 80:20, 62 astrocytes; 70:30, 107 astrocytes). For each simulated culture, we ran 10 simulations. The simulated time was 5 minutes.

Neuronal and astrocytic activity analysis. The sorted signals and the simulated spike trains were further analyzed with a MATLAB tool [19] that uses a network-wide cumulative moving average (CMA) algorithm [9]. We analyzed the spike rate (SR; spikes per minute) and burst rate (BR; bursts per minute) of the recorded and simulated signals. Single-channel SR and BR of the experimental data were then averaged for each MEA. To simulate the capturing of the neuronal activity on an MEA, we randomly selected 64 neurons in the surroundings of the virtual electrode positions. SR and BR of the selected neurons were then determined for the simulated MEA channels. Additionally, we calculated how many times each astrocyte entered the active state during the 5 minutes simulated time. The astrocytes are considered active when the astrocytic intracellular Ca^{2+} overcome a certain threshold and elicit the release of gliotransmitters.

Statistical analysis. Statistical analysis was conducted either in MATLAB or GraphPad Prism (v.9). Firstly, to compare the different experimental and simulated co-cultures, we used a Mann-Whitney *u* test, and the test was considered significant for $p < 0.05$, where p is the probability to obtain results in the tail of the results distribution. A small p-value rejects the null-hypothesis. Secondly, to analyze the correlation between SR or BR and the features from the graph analysis in the experimental data (see paragraph `Graph analysis`), we used Pearson's correlation coefficient *R*. To further test the linear dependence between SR and the degree, we conducted a linear regression analysis (`fitlm`-function in MATLAB). The regression parameter r^2 represents the fraction of data in accordance with the applied regression model. The statistical significance of the regression analysis was tested with a Student's t-test, and the test was considered significant for $p < 0.05$.

Thirdly, to analyze the underlying network structure of the cultures on the MEAs, we conducted a pairwise cross-correlation analysis in MATLAB between binary encoded spike trains of each MEA channel. We created a correlation matrix based on the pairwise correlation values and normalized the matrix by the maximum of all correlation values. We then thresholded the correlation at a value of > 0.65 to consider only the channel pairs with a high positive correlation. We applied the same approach to the selected simulated neuronal spike trains (see paragraph `Neuronal and astrocytic activity analysis`).

Graph analysis. To analyze the structure of the experimental and simulated networks, we conducted an undirected graph analysis on the binary encoded spike trains in MATLAB to measure the network structure of the culture. For this, we evaluated the mean degree of the network, the number of nodes in the network, and the mean shortest path. The edges in this analysis are defined as the connections between the channels (in the experiments) or neurons (in the simulations) with cross-correlation value > 0.65. Nodes were defined as those channels or neurons with at least one edge to another channel or neuron. For the simulated network, we also analyzed the astrocytic structural network by calculating the mean degree and the mean shortest path based on the astrocytic network topology. In this context, the edges were the simulated GJs between astrocytes. Furthermore, we combined the graph analysis from the astrocytic and neuronal networks for the simulated data with the activity analysis (i.e., spike rate).

4 RESULTS

Lower spike rate (SR) and burst rate (BR) in co-cultures. The experimental data showed a higher SR in the NS cultures compared to the co-cultures. Even though only the pairwise comparison between NS and 90:10 was statistically significant ($p = 0.028$), the lower mean SR for the MEAs with astrocytes was noticeable (Fig. 2A). Simulated data of NS also showed a higher SR compared to the simulations with astrocytes comprised in the network (Fig. 2F). In this case, the pairwise differences in SR were significant for NS vs. 90:10 ($p = 0.003$) and NS vs. 80:20 ($p = 0.0015$). Pairwise t-tests between the experimental and simulated data resulted in no statistical difference (NS, $p = 0.67$; 90:10, $p = 0.17$; 80:20, $p = 0.08$; 70:30, $p = 0.83$).

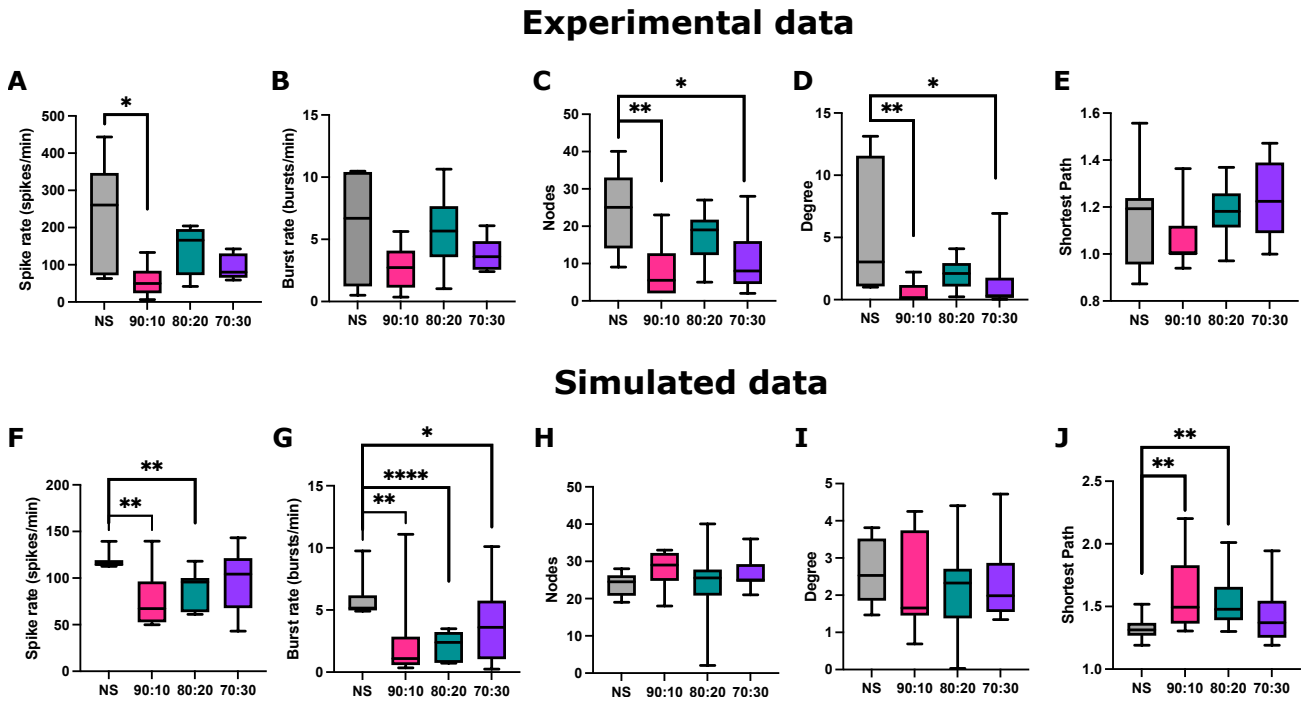

Figure 2: Analysis of the neuronal data. Spike rate (A,F) and burst rate (B,G) as well as the number of nodes (C,H), the mean degree (D,I) and the mean shortest path (E,J) of the experimental data (top panel) and simulated data (bottom panel) for the four culture ratios. Statistical significance: * p<0.05; ** p<0.01; **** p<0.0001.

The mean BR was decreased for all co-cultures compared to NS (Fig. 2B and G). However, those differences were not statistically significant for the experimental data, while they were significant for the simulated data (NS vs. 90:10, p = 0.0027; NS vs. 80:20, p < 0.0001; NS vs. 70:30, p = 0.027). In general, the NS population exhibited very high variability in the experimental data (Fig. 2A and B). In the simulated data, the addition of astrocytes in the network increased the variability of the SR and BR (Fig. 2F and G). The results from the experimental data and the simulations were in similar ranges – the pairwise t-tests gave statistical difference only for the culture ratio 80:20 (NS, p = 0.96; 90:10, p = 0.31; 80:20, p = 0.003; 70:30, p = 0.70).

Graph analysis of the neuronal activity. The graph analysis on the experimental data showed that the NS networks created from the binary encoded spike trains have a higher number of nodes compared to the co-cultures (NS vs. 90:10, p = 0.005; NS vs. 80:20, p = 0.19; NS vs. 70:30, p = 0.03) (Fig. 2C). The number of nodes in the simulated data did not exhibit differences between the culture ratios (Fig. 2H). The simulations reproduced the experimental results for NS but not for the co-cultures. In fact, pairwise comparison between the number of nodes was statistically different for 90:10 and 70:30 (NS, p = 0.94; 90:10, p < 0.0001; 80:20, p = 0.08; 70:30, p = 0.002).

The mean degree was lower in the co-cultures compared to NS in the experimental data (NS vs. 90:10, p = 0.006; NS vs. 80:20, p = 0.28; NS vs. 70:30, p = 0.03) (Fig. 2D). The experimental data indicated more variability in the mean degree of the NS than in the co-cultures. The simulated data did not show significant differences between the cultures (Fig. 2I). The degree values were in the same ranges for the experimental and simulated data for NS and 80:20 but were, however, statistically different for 90:10 and 70:30 (NS, p = 0.65; 90:10, p = 0.0.003; 80:20, p = 0.99; 70:30, p = 0.03).

The mean shortest path for the experimental data was in the same range for NS and the co-cultures, with a tendency to increase with an increasing number of astrocytes in the culture (Fig. 2E). In the simulated data, a decrease in the mean shortest path for the simulated co-cultures was observable (Fig. 2J). Overall, the mean shortest path of the simulated data was slightly higher than the experimental results, and it was statistically different in all the culture ratios except 70:30 (NS, p = 0.03; 90:10, p = 0.0002; 80:20, p = 0.0002; 70:30, p = 0.08).

SR and BR correlation with the graph analysis features of the experimental data. The Pearson's correlation R between the SR and the mean degree was $R = 0.57$ for the NS, $R = 0.03$ for the 90:10, $R = 0.35$ for the 80:20, and $R = 0.27$ for the 70:30 cultures (Fig. 3). The circle diameter represents the degree importance calculated based on the cross-correlation values of the incoming connections. In addition, the linear regression analysis showed that a good agreement between the linear regression and the data was found only for NS, while for the co-cultures the r^2 returned very low values (NS:

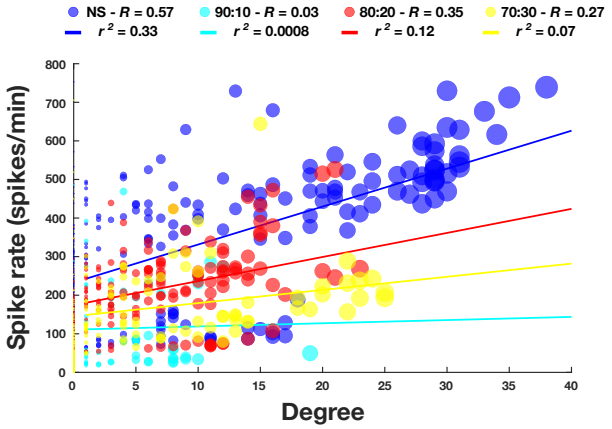

Figure 3: Pearson's correlation analysis *R* between the spike rate and the degree for the four different cultures. Each circle represents one channel of an MEA. The circle diameter represents the node centrality based on cross-correlation values of the incoming edges of the node. The solid lines represent the linear regression models for the experimental data for the different cultures with the relative r^2 parameter.

r^2 = 0.38, p < 0.0001; 90:10: r^2 = 0.0008, p = 0.829; 80:20: r^2 = 0.12, p < 0.0001; 70:30: r^2 = 0.07, p = 0.012).

Graph analysis of the astrocyte topology. For the simulations, we conducted a graph analysis based on the topology of the astrocytes to combine these results with the graph analysis based on the cross-correlation analysis of the simulated neuronal networks. The mean degree and mean shortest path of the astrocytes increased with the number of astrocytes in the network (Fig. 4A and B). All the pairwise differences between the simulated co-cultures were statistically significant (p < 0.0001). The astrocytic activation, expressed as how many times an astrocyte entered the active state during the time of the simulation, instead did not show any differences between the three different simulated co-cultures (Fig. 4C).

Network response to astrocyte influence. For the simulated data, we plotted the structural network based on the graph analysis for the neuronal data with the relative SR of each of the 64 selected neurons indicated by the color bar ranging from blue to green (Fig. 5). The neurons with higher SR are not always those with a higher amount of connections but more centered in the network. The radius of the dot represents the degree of the neurons. The connections here are not the synapses between the neurons but the connections based on the cross-correlation analysis.

To analyze the effect of the astrocytes, we combined the topology network of the astrocytes with the connections determined by the cross-correlation of the binary encoded neuronal activity (Fig. 5). The diamonds represent the astrocytes with their connections, i.e., GJs, and the color of the diamond indicates how many times the astrocyte has been in the active state during the simulation. The dimension of the diamonds reflects the degree of the astrocyte.

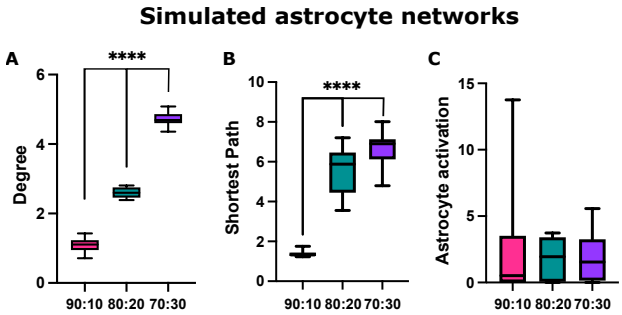

Figure 4: Astrocyte network graph analysis. (A) the mean degree (i.e., gap junctions), (B) the mean shortest path, and (C) the mean number of times an astrocyte entered the active state. The results show the average of the features for the astrocytes in the simulated network. The simulations were repeated ten times for each co-culture. **** **p** < 0.0001.

5 DISCUSSION AND CONCLUSION

Astrocytes have proved to communicate with the neurons and to control the neuronal activity [1–3]. Computational models of astrocytes and neurons can help to highlight the pathway through which this communication happens [12]. Previously, we developed a computational neuron-astrocyte network model called INEXA [11].

In the present work, we aim to analyze how the number of astrocytes and the resulting astrocytic network topology affect neuronal network activity. In the brain, individual areas contain different ratios of neurons and astrocytes [8] and varying numbers of synapses ensheathed by astrocytes [6]. To validate the aim, we ran *in vitro* experiments with MEAs and simulations with the INEXA model side-by-side. We included neuronal cultures without supplemented astrocytes and co-cultures added with different amounts of astrocytes in both setups. Our results from the experimental data show that NS cultures exhibited a high variability which might be due to different maturation stages within those cultures [15, 16]. Compared to the NS cultures, the neuron-astrocyte co-cultures exhibit a lower SR and BR. With our simulations, we can replicate similar SR and BR. Also, the nodes and degree analysis based on the neuronal cross-correlation analysis shows a lower amount of nodes and a lower mean degree for the co-cultures than NS cultures. During the spike sorting of the MEA recordings, we realized that the cultures containing more astrocytes have smaller amplitudes of the action potentials. This might have led to underestimating the spike number (which is beyond the scope of this paper). It is an interesting feature to be investigated in the future.

The Pearson's correlation and linear regression analysis of the experimental data reveals that the SR is correlated with the mean degree for NS and that the correlation coefficient *R* decreased for the co-cultures. These results indicate that the number of astrocytes in the network affects neuronal activity. Since it is very challenging to experimentally study the effect of the astrocytic topology and activation on neuronal network activity, we used our computational model to overcome this limitation. Our results from the graph analysis of the astrocytic network topology show that the mean degree, which represents the number of GJs, and the mean shortest

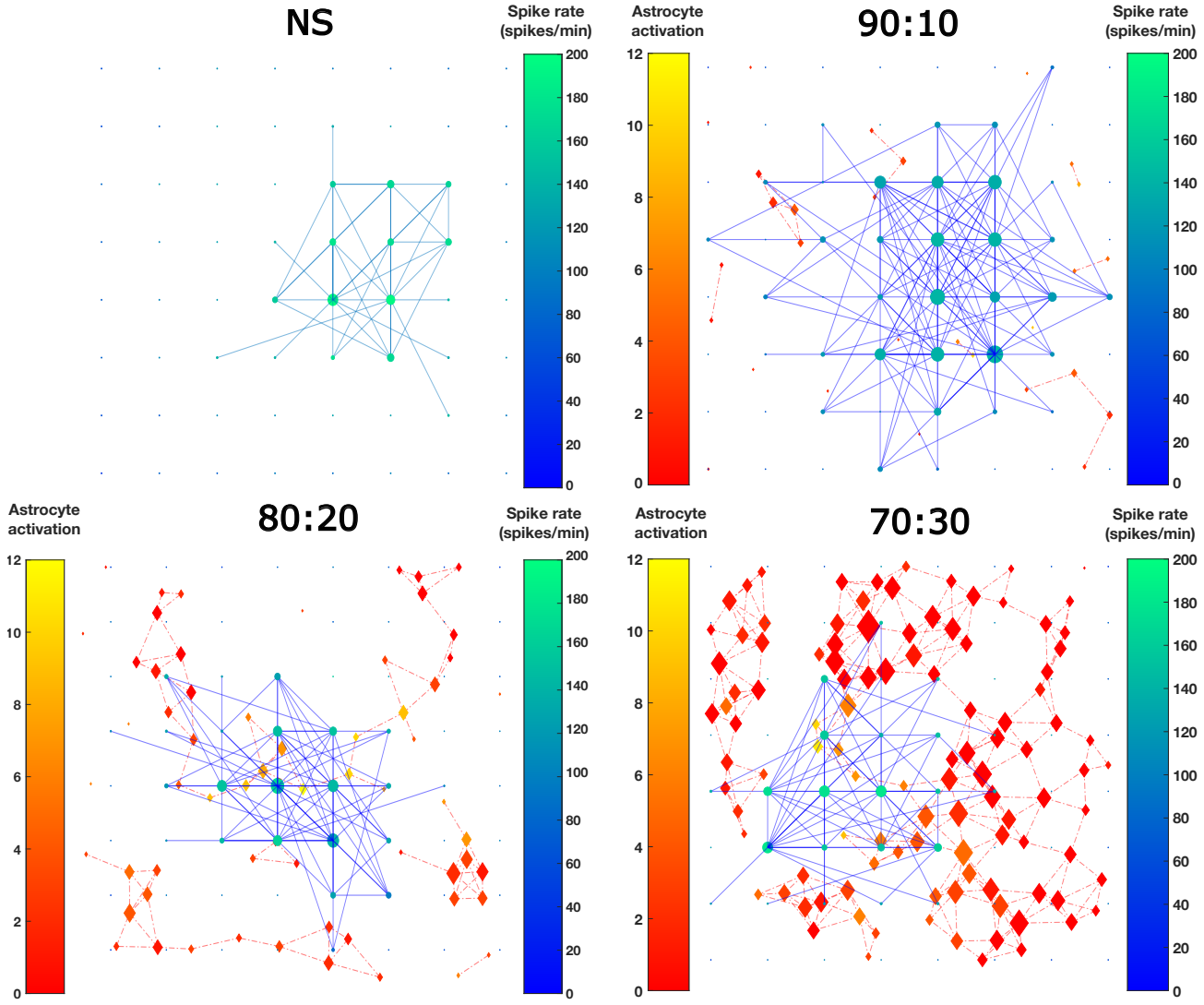

Figure 5: Combination of astrocytic network effect and the neuronal activity network for the simulated data. The 64 selected neurons are shown as dots. The neuronal connections based on the cross-correlation are shown in solid blue lines (edge weight > 0.65). The diameter of the dot reflects the degree of the neuron. The color bar for the SR values (spikes/min) ranges from blue (low) to green (high). The astrocytes are shows in diamond shape and their gap junctions as dot-dashed red lines. The astrocyte activation defines how many times that particular astrocyte got activated; the color bar ranges from red (low) to yellow (high). The dimension of the diamonds reflects the degree of the astrocyte.

path increased when increasing the number of astrocytes in the network. Instead, the astrocytic activation does not differ between the simulated co-cultures showing that the activation through GJs had a low effect. The astrocytes redistribute the resources (i.e., glutamate and IP_3) through the GJs, and they get activated based on these resources. Thus, the more GJs an astrocyte has, the less the distribution has activating effect on the connected astrocytes. This behavior might be indicated by the higher variability in the activation for 90:10. Instead, the variability in the astrocyte activation of the 70:30 culture can be explained by a higher input from the neurons.

To study how the astrocytes locally affect neuronal activity, we combine the cross-correlation-based graph analysis with the astrocyte topology and activation. Highly spiking neurons in our simulated networks are localized in the network center and only slightly depend on the degree. These results from the simulations are following the results from the correlation analysis of the experimental data. The activation of the astrocytes was mainly co-localized with the highly spiking neurons but not dependent on the astrocyte mean degree. However, the increase of neuronal SR with higher numbers of astrocytes seems to depend on the astrocyte mean degree. These results are in accordance with [10] and [7]. In previous

publications, we found that hub astrocytes with a high number of GJs lead to higher SR [7] and centralize the neuronal activity [10]. Also, our results show a feedback communication with neurons and a preferential inhibition in less connected networks.

SOFTWARE AND DATA AVAILABILITY

The code and the resulting data used in this study can be found at https://github.com/barbara-ge/ACM-NanoCom2021. The MATLAB code for the published INEXA model [11] is available in a publicly accessible repository: https://github.com/kerstinlenk/INEXA_FrontCompNeurosci2020. The code for the burst analysis tool is stored at https://doi.org/10.5281/zenodo.3883622.

ACKNOWLEDGEMENT

The authors acknowledge the TUNI TCSC Narvi computing cluster for the computational resources. The work of B.G. and M.T.B. is funded by the European Union's Horizon 2020 Research and Innovation Programme under the Marie Skłodowska-Curie grant agreement No. 713645 and No. 839553. The works of A.A. and J.M.A.T. have been supported by funding from the European Union's Horizon 2020 Research and Innovation Programme under grant agreement No. 824164, project "Hybrid Enhanced Regenerative Medicine Systems". K.L. received funding from the Academy of Finland (decision nos. 314647, 326452).

REFERENCES

[1] Mahmood Amiri, Narges Hosseinmardi, Fariba Bahrami, and Mahyar Janahmadi. 2013. Astrocyte-neuron interaction as a mechanism responsible for generation of neural synchrony: a study based on modeling and experiments. *Journal of Computational Neuroscience* 34, 3 (2013), 489–504. https://doi.org/10.1007/s10827-012-0432-6

[2] Alfonso Araque, Vladimir Parpura, RP Sanzgiri, and PG Haydon. 1999. Tripartite synapses: glia, the unacknowledged partner. *Trends in Neurosciences* 22, 5 (1999), 208–215. https://doi.org/10.1016/s0166-2236(98)01349-6

[3] Paola Bezzi, Giorgio Carmignoto, Lucia Pasti, Sabino Vesce, Daniela Rossi, Barbara Lodi Rizzini, Tullio Pozzant, and Andrea Volterra. 1998. Prostaglandins stimulate calcium-dependent glutamate release in astrocytes. *Nature* 391, 6664 (1998), 281–285. https://doi.org/10.1038/34651

[4] Fernando J. Chaure, Hernan G. Rey, and Rodrigo Quian Quiroga. 2018. A novel and fully automatic spike-sorting implementation with variable number of features. *Journal of Neurophysiology* 120, 4 (2018), 1859–1871. https://doi.org/10.1152/jn.00339.2018 PMID: 29995603.

[5] Elena Dossi, Flora Vasile, and Nathalie Rouach. 2018. Human astrocytes in the diseased brain. *Brain Research Bulletin* 136 (2018), 139–156. https://doi.org/10.1016/j.brainresbull.2017.02.001 Molecular mechanisms of astrocyte-neuron signalling.

[6] Isabella Farhy-Tselnicker and Nicola J. Allen. 2018. Astrocytes, neurons, synapses: A tripartite view on cortical circuit development. *Neural Development* 13, 1 (2018), 1–12. https://doi.org/10.1186/s13064-018-0104-y

[7] Barbara Genocchi, Kerstin Lenk, and Jari Hyttinen. 2020. Influence of Astrocytic Gap Junction Coupling on in Silico Neuronal Network Activity. In *MEDICON 2019, IFMBE Proceedings*. Springer Nature Switzerland AG 2020, 480–487. https://doi.org/10.1007/978-3-030-31635-8

[8] Suzana Herculano-Houzel. 2014. The glia/neuron ratio: How it varies uniformly across brain structures and species and what that means for brain physiology and evolution. *Glia* 62, 9 (2014), 1377–1391. https://doi.org/10.1002/glia.22683

[9] Fikret Emre Kapucu, Jarno Tanskanen, Jarno Mikkonen, Laura Ylä-Outinen, Susanna Narkilahti, and Jari Hyttinen. 2012. Burst analysis tool for developing neuronal networks exhibiting highly varying action potential dynamics. *Frontiers in Computational Neuroscience* 6 (2012), 38. https://doi.org/10.3389/fncom.2012.00038

[10] Kerstin Lenk, Barbara Genocchi, Michael T Barros, and Jari A.K. Hyttinen. 2021. Larger Connection Radius Increases Hub Astrocyte Number in a 3D Neuron-Astrocyte Network Model. *IEEE Transactions on Molecular, Biological and Multi-Scale Communications* (2021), 1–5. https://doi.org/10.1109/TMBMC.2021.3054890

[11] Kerstin Lenk, Eero Satuvuori, Jules Lallouette, Antonio Ladrón-de Guevara, Hugues Berry, and Jari A. K. AK Hyttinen. 2020. A Computational Model of Interactions Between Neuronal and Astrocytic Networks: The Role of Astrocytes in the Stability of the Neuronal Firing Rate. *Frontiers in Computational Neuroscience* 13, January (2020), 92. https://doi.org/10.3389/fncom.2019.00092

[12] Franziska Oschmann, Hugues Berry, Klaus Obermayer, and Kerstin Lenk. 2017. From in silico astrocyte cell models to neuron-astrocyte network models: A review. *Brain Research Bulletin* 136 (2017), 1–9. https://doi.org/10.1016/j.brainresbull.2017.01.027

[13] Gertrudis Perea and Alfonso Araque. 2007. Astrocytes potentiate transmitter release at single hippocampal synapses. *Science (New York, N.Y.)* 317, 5841 (2007), 1083–6. https://doi.org/10.1126/science.1144640

[14] Mirko Santello, Nicolas Toni, and Andrea Volterra. 2019. Astrocyte function from information processing to cognition and cognitive impairment. *Nature Neuroscience* 22, 2 (2019), 154–166. https://doi.org/10.1038/s41593-018-0325-8

[15] George M. Smith, Urs Rutishauser, Jerry Silver, and Robert H. Miller. 1990. Maturation of astrocytes in vitro alters the extent and molecular basis of neurite outgrowth. *Developmental Biology* 138, 2 (1990), 377–390. https://doi.org/10.1016/0012-1606(90)90204-V

[16] Arens Taga, Raha Dastgheyb, Christa Habela, Jessica Joseph, Jean-Philippe Richard, Sarah K. Gross, Giuseppe Lauria, Gabsang Lee, Norman Haughey, and Nicholas J. Maragakis. 2019. Role of Human-Induced Pluripotent Stem Cell-Derived Spinal Cord Astrocytes in the Functional Maturation of Motor Neurons in a Multielectrode Array System. *STEM CELLS Translational Medicine* 8, 12 (dec 2019), 1272–1285. https://doi.org/10.1002/sctm.19-0147

[17] Michael Taynnan Barros, Sasitharan Balasubramaniam, and Brendan Jennings. 2015. Comparative End-to-End Analysis of Ca 2+ -Signaling-Based Molecular Communication in Biological Tissues. *IEEE Transactions on Communications* 63, 12 (2015), 5128–5142. https://doi.org/10.1109/TCOMM.2015.2487349

[18] Gaetano Valenza, Luciano Tedesco, Antonio Lanata, Danilo De Rossi, and Enzo P asquale Scilingo. 2013. Novel Spiking Neuron-Astrocyte Networks based on nonlinear transistor-like models of tripartite synapses. *Conference Proceedings of the Annual International Conference of the IEEE EMBS* (2013), 6559–6562. https://doi.org/10.1109/EMBC.2013.6611058

[19] Inkeri A. Välkki, Kerstin Lenk, Jarno E. Mikkonen, Fikret E. Kapucu, and Jari A. K. Hyttinen. 2017. Network-Wide Adaptive Burst Detection Depicts Neuronal Activity with Improved Accuracy. *Frontiers in Computational Neuroscience* 11 (2017), 40. https://doi.org/10.3389/fncom.2017.00040